Probing Single-Molecule Dissociations from a Bimolecular Complex NO—Co-Porphyrin

Howon Kim,[†,#] Yun Hee Chang,[‡,#] Won-Jun Jang,[†] Eui-Sup Lee,[‡] Yong-Hyun Kim,[*,‡] and Se-Jong Kahng[*,†]

[†]Department of Physics, Korea University, 1-5 Anam-dong, Seongbuk-gu, Seoul, 136-713, Republic of Korea and [‡]Graduate School of Nanoscience and Technology, KAIST, Daejeon 305-701, Republic of Korea. [#]These authors contributed equally.

ABSTRACT Axial coordinations of diatomic NO molecules to metalloporphyrins play key roles in dynamic processes of biological functions such as blood pressure control and immune response. Probing such reactions at the single molecule level is essential to understand their physical mechanisms but has been rarely performed. Here we report on our single molecule dissociation experiments of diatomic NO from NO—Co-porphyrin complexes describing its dissociation mechanisms. Under tunneling junctions of scanning tunneling microscope, both positive and negative energy pulses gave rise to dissociations of NO with threshold voltages, +0.68 and −0.74 V at 0.1 nA tunneling current on Au(111). From the observed power law relations between dissociation rate and tunneling current, we argue that the dissociations were inelastically induced with molecular orbital resonances by stochastically tunneling electrons, which is supported with our density functional theory calculations. Our study shows that single molecule dissociation experiments can be used to probe reaction mechanisms in a variety of axial coordinations between small molecules and metalloporphyrins.

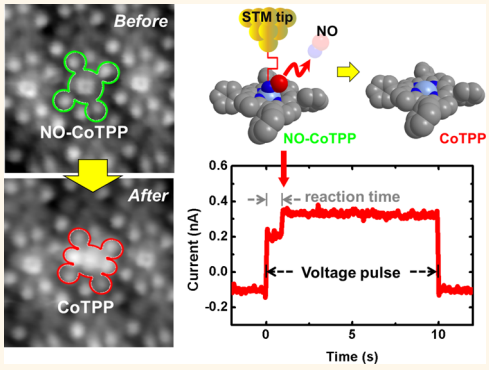

KEYWORDS: scanning tunneling microscopy · density functional theory · metalloporphyrin · nitric oxide · bimolecular reaction · dissociation

The toxic compound nitric oxide (NO) is involved in a variety of biological functions such as nerve-signal transduction, dilation of blood vessel, and immune response.[1−3] An essential part of its activation process is axial coordination (dissociation) of NO to (from) the metal center of metalloporphyrin. NO coordination weakens the molecular ligand opposite to NO in six coordinated metal structures to trigger subsequent structural transformations and reactions. The coordination and dissociation between small molecules (NO, O_2, and CO) and metallo-porphyrins are also useful to control spin-configurations of metalloporphyrin systems with potential applications in molecular sensing and spintronic devices.[4−8] Physical kinetics of NO coordination and dissociation has been widely studied for the last two decades, and its reaction rate constants and activation parameters were revealed with various techniques including laser flash photolysis.[9] In such a method, NO is dissociated from NO—metalloporphyrin in solution phases through photoinduced dissociations. In analogy with photoinduced mechanisms, electron-induced dissociation of NO from NO—metalloporphyrin complexes can also take place and be used to study its reaction kinetics in a vacuum environment. This method can be implemented with scanning tunneling microscopy (STM) that allows studies at the single molecule level, in contrast to laser photolysis that probes ensembles of molecules. However, the study that quantitatively correlates the single molecule dissociation experiments of NO with its reaction mechanisms has been rare in the literature.[10−12]

In this paper, we present experimental results of single molecule dissociations of NO from NO—Co-tetraphenylporphyrin (NO—CoTPP) complexes, and propose its dissociation mechanisms. Under tunneling junction of STM, we observed that the dissociations of NO took place with voltage pulses higher (lower) than +0.68 (−0.74) V

* Address correspondence to yong.hyun.kim@kaist.ac.kr, sjkahng@korea.ac.kr.

Received for review June 8, 2015 and accepted July 14, 2015.

Published online July 14, 2015
10.1021/acsnano.5b03466

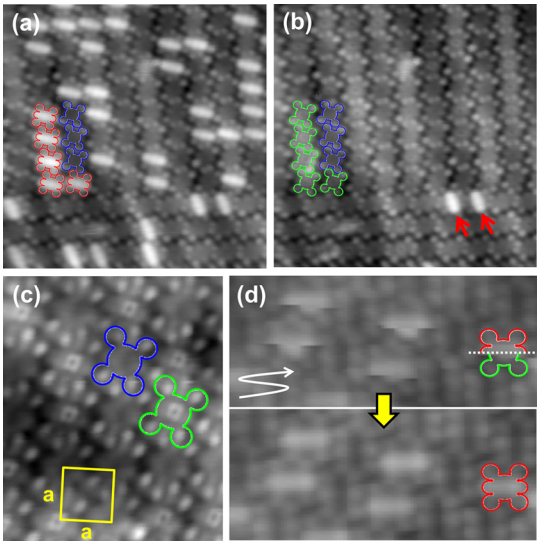

Figure 1. STM images of mixed CoTPP and H_2TPP on Au(111) (a) before and (b, c) after exposure to 300 L of NO gas. The tunneling conditions are I_T = 0.1 nA and V_S = −0.6 eV. Two CoTPP molecules which are not affected by NO-exposure were marked with red arrow in panel b. A molecular unit cell is depicted as a yellow square with a lattice constant a = 1.40 ± 0.01 nm in panel c. (d) STM images showing NO dissociations (top) during scaning with V_S = −1.0 eV. (bottom) Five NO−CoTPPs become CoTPPs after scanning the area. The scanning direction is depicted as an arrow in the upper STM image. The dotted line indicates a sudden transition from NO−CoTPP to CoTPP. For clarity, the three representative molecules of CoTPP, H_2TPP, and NO−CoTPP are denoted by red, blue, and green marks, respectively, in all STM images. Size of images: (a, b) 14.0 × 14.0 nm^2, (c) 6.5 × 7.0 nm^2.

at 0.1 nA tunneling current on Au(111). The observed dissociations were explained with inelastically induced molecular orbital resonances and Arrhenius equations with Gibbs free energy, based on our density functional theory (DFT) calculations.

RESULTS AND DISCUSSION

We deposited a mixture of CoTPP and H_2TPP on Au(111) at 150 K. Two different molecules formed square grid islands with random occupation and could be distinguished in STM images by the shapes of their central bodies, macrocycles with Co or H_2. CoTPP has a three-lobed structure with a bright center due to Co in STM images, whereas H_2TPP has a dark ring with center depression due to an absent electronic state.[12−19] These molecular islands were exposed to NO gas at 80 K with the STM tip retracted. Figure 1 panels a and b show the STM images obtained from the same area before and after 300 L exposure of NO gas, respectively. The shapes of H_2TPPs were not affected by NO exposure, whereas about 40% of CoTPPs were changed from the three-lobed structures to bright ring shapes as shown in Figure 1c. We assigned the bright rings as the structures of NO−CoTPP nitrosyl complex.

The STM images shown in Figure 1b were obtained at sample voltage V_S = −0.6 V and tunneling current

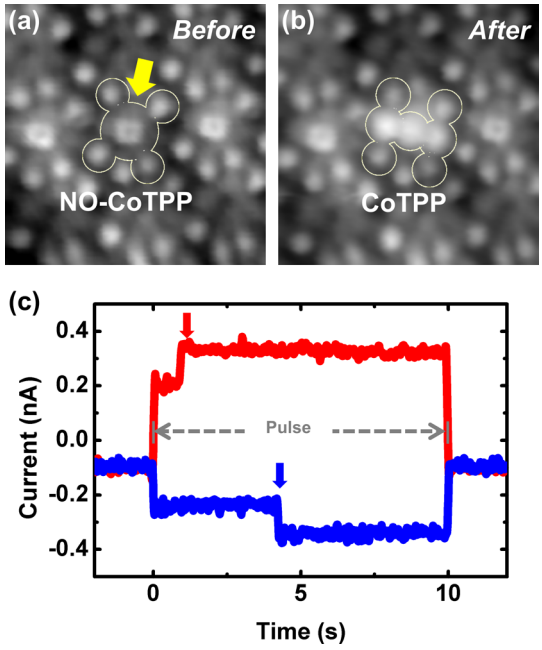

Figure 2. STM images obtained (a) before and (b) after a voltage pulse manipulation. (c) Two examples of tunneling currents measured during voltage pulse manipulations. In both cases, tunneling current jumped three times. The first and the third jumps are the results of applied voltage pulses, and the second jump is indicative of NO dissociation. The duration time between the first and second is a reaction time, which is used for obtaining the dissociation rate as a function of tunneling current in Figure 3b.

I_T = 0.1 nA. When the sample voltage was changed to −1.0 V, we often observed that the molecules of bright ring shapes were changed back to three-lobed structures as shown in Figure 1d. This means that NO was dissociated from NO−CoTPP with electron-tunneling induced mechanisms. Dissociated NO molecules seemed to desorb to vacuum and were not found near CoTPP on the surface. We also observed similar dissociation behaviors at +1.0 V. We quantified these observations by measuring dissociation rates and probabilities at different voltages and tunneling currents. To do that, we used a voltage pulse manipulation for each dissociation experiment; we located the STM tip at the center of NO−CoTPP, turned off the feedback loop, applied a voltage pulse for 10 s duration, and monitored tunneling current. Figure 2 panels a and b show two STM images obtained before and after a voltage pulse manipulation, respectively, which show a clear shape change in a molecule. Figure 2c shows a tunneling current monitored during two different manipulations with positive (+0.8 V, red) and negative (−0.8 V, blue) voltage pulses. In both cases, the tunneling current jumped three times. The first and the third jumps are the results of applied voltage pulses, and the second jump is the indicative of NO dissociation. The duration time between the first and second is an electron exposure time or a reaction time, which can be converted to the reaction rate for each manipulation.

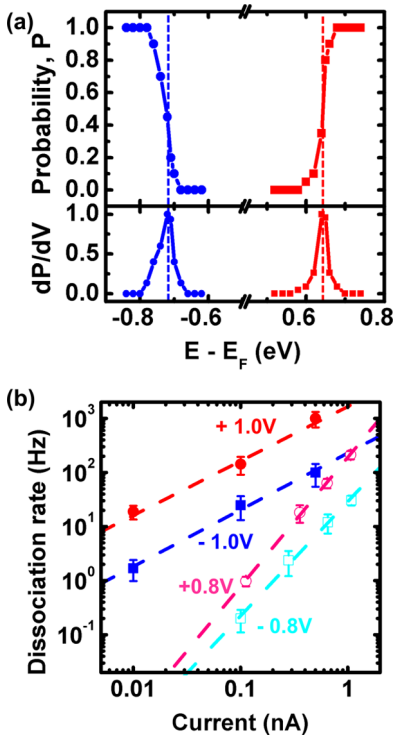

Figure 3. (a) Average dissociation probability (*P*) and d*P*/d*V* for 10 s pulse duration measured at different sample voltages with the tunneling current 0.1 nA for 520 different NO−CoTPPs. Two dotted lines guide the eyes for two peaks which are related to the threshold voltages of NO dissociations in the d*P*/d*V* plot. (b) Time durations for dissociations measured at sample voltages +1.0, +0.8, −0.8, and −1.0 V, and plotted with tunneling currents.

We repeated the voltage pulse manipulations on ten different NO−CoTPPs for each tunneling condition.

The average dissociation probability (*P*) for 10 s pulse durations is measured at different sample voltages with the tunneling current of 0.1 nA, as shown in Figure 3a. We were able to determine threshold voltages for dissociations at both polarities, +0.68 and −0.74 V, from d*P*/d*V* analysis. We also measured dissociation rates at different tunneling currents for ±0.8 and ±1.0 V voltage pulses as shown in Figure 3b. There have been reports that described small molecule dissociation from metalloporphyrins and phthalocyanins with either electric field induced mechanisms or inelastic tunneling mechanisms.[10−12,20] In fact, we tried to perform the same experiments at even higher voltages such as at $V_S \geq |1.5|$ V. However, the dissociation of NO took place in a group of complexes rather than a single NO−CoTPP complex at such high voltages. This might be caused by electric field-induced chemical reaction. In our experiments, the bond-breaking yields were independent of electric field at $V_S \leq |1.0|$ V, therefore we tend to consider the NO dissociation mechanism as bond breaking by inelastic electron tunneling through molecular orbital resonances.[21−29] A signature of such mechanisms is the power law dependency of the reaction rate (*R*) on the tunneling current (*I*), that is, $R \propto I^N$, where *N* is the order of reaction. We fit our data to the power law dependency as in Figure 3b, and obtained the reaction rate proportional to $I^{1.0\pm0.2}$, $I^{2.3\pm0.1}$, $I^{2.1\pm0.1}$ and $I^{1.0\pm0.2}$ at the sample voltages +1.0, +0.8, −0.8, and −1.0 V, respectively. This could be interpreted that one (two) electron is involved in the dissociation processes at $|V| = 1.0$ V ($|V| = 0.8$ V) with a dissociation rate of 0.1−1000 Hz for tunneling currents of 0.01−1 nA. Note that the reaction rates are lower (by a factor of 10) at negative bias voltages than those at positive.

To microscopically understand the NO dissociation mechanics, we performed first-principles density-functional theory (DFT) calculations for NO−CoTPP on Au(111) using the Vienna *ab initio* simulation package (VASP).[30] To evaluate first-principles thermodynamics of the NO dissociation, we considered not only adsorption−desorption energetics, zero-point energy, and vibrational free energy at experimental temperature from first-principles, but also the chemical potential of NO gas from experiment at the cryogenic ultra-high vacuum condition.[31] In DFT calculations, a kinetic energy cutoff of 400 eV for the plane-wave expansion, projected augmented wave (PAW) potentials,[32] and Perdew−Burke−Ernzerhof (PBE)[33] exchange-correlation functional with and without van der Waals correction[34] were used. For the Au(111) surface, we used a p(6×6) surface slab model with three atomic layers. The standard NO chemical potential was obtained from the thermochemical table[35,36] and fitted with polynomials [see Supporting Information].

The NO dissociation takes place both at positive and negative bias voltages (V_{bias}) in experiment. Therefore, an excessvie energy, $e|V_{bias}|$, of hot tunneling electrons may be transferred to the vibrational energy of NO molecules by inelastic electron tunneling through molecular orbitals of NO in occupied and unoccupied states. To see the presence of such molecular orbitals, we analyzed the electronic structure, particularly the local density of states, of NO-adsorbed CoTPP on Au(111), as shown in Figure 4b. When we do not consider the van der Waals (vdW) correction in DFT-PBE calculations, the highest occupied molecular orbital (HOMO) of NO−CoTPP locates at 0.1 eV below the Fermi energy (E_F), and the lowest unoccupied molecular orbital (LUMO) of NO−CoTPP/Au(111) locates at 1.4 eV above E_F. When we include the vdW correction in calculations, the whole molecular orbitals of NO−CoTPP are down-shifted, and E_F locates almost in the middle of the HOMO-LUMO gap. The rigid shift of molecular orbitals is due to electron transfer from NO−CoTPP to Au(111), as shown in Figure 4c.[37] If we compress down the NO−CoTPP molecule more to the Co−Au distance of 3.16 Å, the HOMO (LUMO) locates 0.8 eV (0.7 eV) below (above) E_F, roughly agreeing with experimental on-set voltages of NO dissociation. This supports that the dissociations of NO both at positive

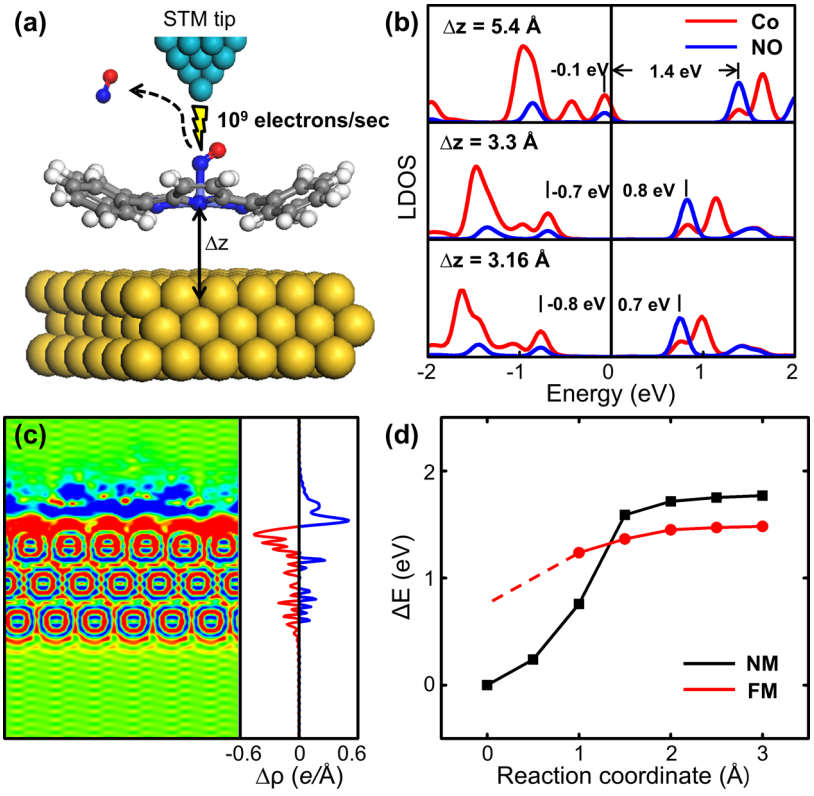

Figure 4. (a) Schematic of NO dissociation from NO−CoTPP/Au(111) due to an electric pulse from STM tip. Δz represents the separation between the Co atom and the top Au atomic layer. (b) Site-projected local density of states (LDOS) for NO−CoTPP/Au(111) from DFT-PBE calculations (top) without dispersion correction, (middle) with dispersion correction, and (bottom) with a compressed configuration. (c) Contour and line plots of integrated charge transfer from NO−CoTPP to Au(111), representing a development of the surface dipole field. (d) Potential energy surface of NO dissociation from NO−CoTPP/Au(111). Nonmagnetic (NM) and ferromagnetic (FM) spin configurations between NO and CoTPP were considered.

and negative bias voltages are caused by molecular orbital resonances. In our previous work, we used the voltage ramp method to induce dissociation of NO from CoTPP.[18] During the voltage ramp, we monitored tunneling current and observed sudden change near $|V| = 0.7$ V. We obtained similar threshold voltages in the two methods, voltage ramp and pulse methods, at similar tunneling currents. The observed consistency implies that the dissociation mechanisms in two methods are the same, the orbital-resonance tunneling.

To find the reaction energy barrier, we considered nonmagnetic and ferromagnetic spin configurations between NO and CoTPP/Au(111) in vdW-corrected DFT-PBE calculations and obtained potential energy surfaces as a function of NO dissociation reaction coordinate, as shown in Figure 4d. We could see that, for NO dissociation, spin flip (and thus charge transfer from NO to CoTPP) should occur at the NO−Co displacement of about 1.9 Å. Also, it appears that there is no additional energy barrier to overcome for NO dissociation other than the NO adsorption energy, which was calculated to be 1.50 eV. Still, the 0.8 or 1.0 eV energies carried by tunneling electrons in experiments may not be enough to overcome the calculated barrier. Thus, we believe the free energy change ΔG should be more relevant for NO adsorption-dissociation mechanics than the adsorption energy change ΔE for these vacuum experiments, as represented,[31]

$$\Delta G(T,P) = \Delta E + \Delta \mathrm{ZPE} + \Delta F(T) + \mu^0_{\mathrm{NO}}(T) + k_B T \ln(P/P_0) \quad (1)$$

where the variation ΔG was taken as G(desorbed) − G(adsorbed) in view of the NO dissociation, ΔE = 1.50 eV. The zero-point energy correction ΔZPE and vibrational free-energy correction ΔF were calculated to be −0.08 and 0.003 eV, respectively, from DFT-PBE vibrational spectra; the NO chemical potential μ^0_{NO} at 80 K and 1 atm was estimated as −0.12 eV, and the logarithmic term with $k_B T$ for a NO partial pressure of 10^{-10} Torr is −0.20 eV. Therefore, ΔG = 1.10 eV, which is the first-principles reaction energy barrier for the NO dissociation at 80 K and 10^{-10} Torr.

At the tunneling currents of 0.01−1 nA, 10^8−10^{10} electrons per second tunnel through the vacuum barrier between the tip and NO−CoTPP/Au(111), and the tunneling electrons dissociate NO molecules to vacuum at a frequency of 0.1−1000 Hz when an enough bias voltage is applied. As the energies of vibrational modes of coordinated NO in this dissociation are several tens of meV (see Supporting Information), a tunneling electron induces excitations of

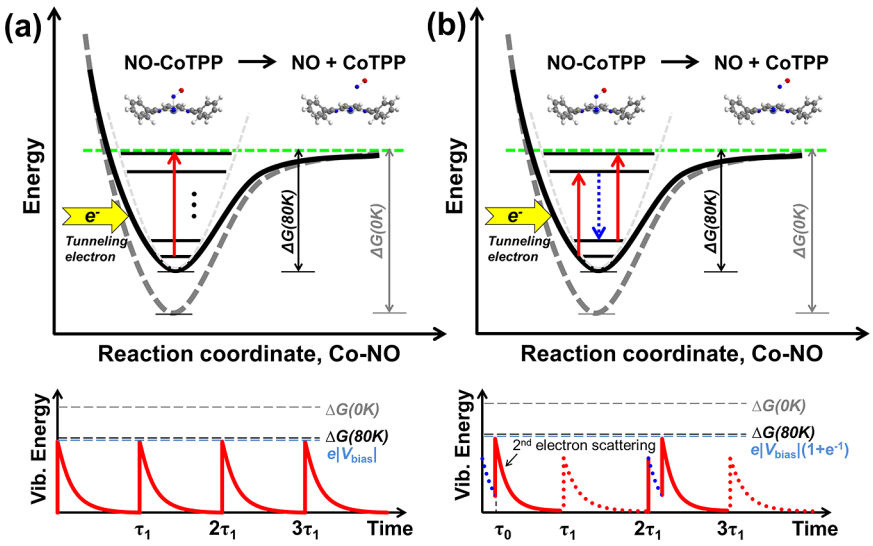

Figure 5. Mechanisms of resonant dissociation by tunneling electrons for (a) one- and (b) two-electron processes. The thick solid line (thick dotted) is corrected (not corrected) potential energy profile based on calculations with a dissociation barrier. The resonant absorption of the tunneling electron with $e|V_{bias}|$ generates the vibrational modes associated with Co-NO (red, (a and b)). The kinetic energy of the hot electrons is transferred into intramolecular vibrational thermal energy and results in NO dissociation. A relaxation of excited vibration modes is denoted as dotted arrow (blue) in panel b. (bottom) Schematic of vibrational energy profiles as a function of time, showing an energy transfer by inelastic scattering with tunneling electrons and a rapid cooling process, compared with the dissociation energy barrier, ΔG: (a) one-electron scattering process by regular tunneling electrons and (b) two-electron process by irregular tunneling electrons with an excessive energy, $e|V_{bias}|$. τ_1 is the average arrival time (e/I) of tunneling electrons at a tunneling current I.

multiple modes.[21−23,27] Because the reaction energy barrier for the NO dissociation is ΔG = 1.10 eV, the dissociation rate can be determined by the Arrhenius equation. To quantitatively understand the NO dissociation rate, we classified several time-scales that are involved in the tunneling-induced NO dissociation. In a resonant tunneling of hot electron through molecular orbitals (HOMO/LUMO), an electron occupies an excited state of the NO−CoTPP complex with a residence time of a femtosecond. During this time, the energy of electron is transferred to all the available vibrational modes (multivibration mode excitations below the V_s) of the complex. Then, the energy of excited vibration modes dissipates to the vibrational relaxation (or cooling down), which is on the order of pico-seconds (τ_0). Also, tunneling electrons arrive at every nanosecond (τ_1) on average. Figure 5 shows schematics describing dissociation mechanisms and vibrational energy profiles as a function of time, compared with the reaction energy barrier ΔG, involving (a) one- and (b) two-tunneling electron process. If the V_S is greater than the reaction energy barrier, the dissociation can take place by a single electron excitation (n = 1). If the V_S is smaller than the barrier, single excitation is not enough to overcome the barrier, as a result the second electron is necessary within a lifetime of the first excitation (n = 2). In any cases, the energy required for dissociation can be estimated by fitting the experimental reaction rate *versus* current to the Arrhenius equations. A probability of multielectron-vibration mode scattering could be represented as $(\tau_0/\tau_1)^{n-1}$ assuming stochastically tunnelling electrons. Then, the Arrhenius equation for the NO dissociation by n-electrons can be expressed as

$$R(n) = 1/(n\tau_1)(\tau_0/\tau_1)^{n-1} \exp[-(\Delta G - \gamma e|V_{bias}|)/k_B T] \quad (2)$$

where $\gamma e|V_{bias}|$ represents an amount of energy transferred by n-electron scattering at V_{bias}. For instance, the second electron should arrive before the first excited vibrational mode is cooled down for two-electron-vibration mode scattering, of which the probability would be τ_0/τ_1, as shown in Figure 5b. Then, the maximum of the excited vibrational energy would be $e|V_{bias}|(1 + 1/e) = 1.37\ e|V_{bias}|$. We fitted the experimental data to eq 2 using τ_0 = 10 ps and γ as a fitting parameter, and obtained γ = 1.0 for one-electron scattering (100% energy transfer) and γ = 1.26 for two-electron scattering [see Supporting Information], which means that for two-electron scattering, 26% energy of first electron is used to NO dissociation in addition to the energy of the second electron. The energy transfer at the high bias voltages of ±1.0 V may be less effective because of a poorer scattering cross-section with molecular orbitals at around ±0.8 eV. Our theoretical analysis suggested that the stochasticity of correlations in energy transfer between the injected electrons give rise to the observed power-law dependency in two different processes in the dissociative reactions. Therefore, we propose that eq 2 quantitatively represents the microscopic dissociation mechanics of

NO molecules from NO−CoTPP/Au(111) by stochastically tunneling electrons.

CONCLUSION

In summary, we studied single molecule dissociations of diatomic NO from NO−CoTPP complexes using STM on Au(111). Under tunneling junctions, dissociations of NO were induced by both positive and negative voltage pulses with threshold voltages, +0.68 and −0.74 V, respectively, at 0.1 nA tunneling current. Tunneling-current dependent yield revealed that a dissociation event required two electrons at $|V| = 0.8$ V and one electron at $|V| = 1.0$ V. Using first-principles thermodynamics for the NO dissociation, the dissociations were induced with inelastic electron tunneling through molecular orbital resonances. Our study can be extended to a variety of coordination complexes between small molecules (NO, O_2, CO, H_2O, NH_3, etc.) and metalloporphyrins (FeTPP, NiTPP, etc.) being used to extract kinetic parameters through single molecule level experiments. The binding configurations of small molecules to the other metalloporphyrins are quite different from NO−CoTPP. Different occupation of valence electrons at the transition metal center may lead to different binding structures and dissociation mechanisms.

EXPERIMENTAL SECTION

All STM experiments were performed in our home-built ultrahigh vacuum (UHV) system operating at 80 K with a base pressure of 1×10^{-10} Torr. The Au(111) surface was prepared from a commercially available thin film (200 nm thick, PHASIS, Switzerland) of Au on mica that was cleaned by several cycles of Ne-ion sputtering followed by annealing at 800 K. Commercially available CoTPP (Porphyrin Systems, Germany) and H_2TPP (Sigma-Aldrich, USA) were degassed in vacuum for several hours prior to all deposition experiments and then deposited on the Au(111) at submonolayer coverage by thermal evaporation using an alumina-coated evaporator. After deposition of CoTPP and H_2TPP onto the Au(111) surface at 150 K, the sample was transferred into STM and cooled down to 80 K. The sample cleanliness was checked by imaging the surface using a Pt−Rh STM tip before exposing the NO gas onto the sample. The NO gas was introduced using a stainless steel tube (3 mm diameter) which is aligned directly onto the sample holder through a precision leak valve.

Conflict of Interest: The authors declare no competing financial interest.

Acknowledgment. The authors gratefully acknowledge financial support from the National Research Foundation of Korea (Grant Nos. 2012-01013222; 2014-11051782). Work at KAIST was supported by the NRF (2012R1A2A2A01046191) and Global Frontier R&D (2011-0031566: Center for Multiscale Energy Systems) programs.

Supporting Information Available: Chemical potential of nitric oxide (NO) gas; NO vibration modes calculation; NO dissociation rate by *n*-electron scattering. The Supporting Information is available free of charge on the ACS Publications website at DOI: 10.1021/acsnano.5b03466.

REFERENCES AND NOTES

1. Kadish, K. M.; Smith, K. M.; Guilard, R. *The Porphyrin Handbook*; Academic Press: New York, 1999.
2. Hoshino, M.; Laverman, L.; Ford, P. C. Nitric Oxide Complexes of Metalloporphyrins: An Overview of Some Mechanistic Studies. *Coord. Chem. Rev.* **1999**, *187*, 75–102.
3. Ford, P. C.; Lorkovic, I. M. Mechanistic Aspects of the Reactions of Nitric Oxide with Transition-Metal Complexes. *Chem. Rev.* **2002**, *102*, 993–1018.
4. Ignarro, L. J. *Nitric Oxide: Biology and Pathobiology*, 1st ed.; Academic Press: San Diego, 2000.
5. Cotton, F. A.; Wilkinson, G.; Murillo, C. A.; Bochmann, M. *Advanced Inorganic Chemistry*, 6th ed.; Wiley-Interscience: 1999.
6. Huheey, J. E.; Keiter, E. A.; Keiter, R. L. *Inorganic Chemistry: Principles of Structure and Reactivity*, 4th ed.; Prentice Hall: **1997**.
7. Flechtner, K.; Kretschmann, A.; Steinrück, H. P.; Gottfried, J. M. NO-Induced Reversible Switching of the Electronic Interaction between a Porphyrin-Coordinated Cobalt Ion and a Silver Surface. *J. Am. Chem. Soc.* **2007**, *129*, 12110–12111.
8. Wäckerlin, C.; Chylarecka, D.; Kleibert, A.; Müller, K.; Iacovita, C.; Nolting, F.; Jung, T. A.; Ballav, N. Controlling Spins in Adsorbed Molecules by a Chemical Switch. *Nat. Commun.* **2010**, *1*, 61.
9. Wanat, A.; Wolak, M.; Brindell, M.; van Eldik, R.; Stochel, G. Laser Flash Photolysis as Tool in the Elucidation of the Nitric Oxide Binding Mechanism to Metallobiomolecules. *Coord. Chem. Rev.* **2002**, *229*, 37–49 and references therein. .
10. Stróżecka, A.; Soriano, M.; Pascual, J.; Palacios, J. Reversible Change of the Spin State in a Manganese Phthalocyanine by Coordination of CO Molecule. *Phys. Rev. Lett.* **2012**, *109*, 147202.
11. Liu, L.; Yang, K.; Jiang, Y.; Song, B.; Xiao, W.; Li, L.; Zhou, H.; Wang, Y.; Du, S.; Ouyang, M.; et al. Reversible Single Spin Control of Individual Magnetic Molecule by Hydrogen Atom Adsorption. *Sci. Rep.* **2013**, *3*, 1210.
12. Burema, S. R.; Seufert, K.; Auwärter, W.; Barth, J. V.; Bocquet, M.-L. Probing Nitrosyl Ligation of Surface-Confined Metalloporphyrins by Inelastic Electron Tunneling Spectroscopy. *ACS Nano* **2013**, *7*, 5273–5281.
13. Seufert, K.; Auwärter, W.; Barth, J. V. Discriminative Response of Surface-Confined Metalloporphyrin Molecules to Carbon and Nitrogen Monoxide. *J. Am. Chem. Soc.* **2010**, *132*, 18141–18146.
14. Auwärter, W.; Seufert, K.; Klappenberger, F.; Reichert, J.; Weber-Bargioni, A.; Verdini, A.; Cvetko, D.; Dell'Angela, M.; Floreano, L.; Cossaro, A.; et al. Site-Specific Electronic and Geometric Interface Structure of Co-Tetraphenyl-Porphyrin Layers on Ag(111). *Phys. Rev. B: Condens. Matter Mater. Phys.* **2010**, *81*, 245403.
15. Scudiero, L.; Barlow, D. E.; Mazur, U.; Hipps, K. W. Scanning Tunneling Microscopy, Orbital-Mediated Tunneling Spectroscopy, and Ultraviolet Photoelectron Spectroscopy of Metal(II) Tetraphenylporphyrins Deposited from Vapor. *J. Am. Chem. Soc.* **2001**, *123*, 4073–4080.
16. Seufert, K.; Bocquet, M. L.; Auwärter, W.; Weber-Bargioni, A.; Reichert, J.; Lorente, N.; Barth, J. V. Cis-Dicarbonyl Binding at Cobalt and Iron Porphyrins with Saddle-Shape Conformation. *Nat. Chem.* **2011**, *3*, 114–119.
17. Kim, H.; Son, W.-j.; Jang, W. J.; Yoon, J. K.; Han, S.; Kahng, S.-J. Mapping the Electronic Structures of a Metalloporphyrin Molecule on Au(111) by Scanning Tunneling Microscopy and Spectroscopy. *Phys. Rev. B: Condens. Matter Mater. Phys.* **2009**, *80*, 245402.
18. Kim, H.; Chang, Y. H.; Lee, S.-H.; Kim, Y.-H.; Kahng, S.-J. Switching and Sensing Spin States of Co−Porphyrin in Bimolecular Reactions on Au(111) Using Scanning Tunneling Microscopy. *ACS Nano* **2013**, *7*, 9312–9317.

19. Kim, H.; Chang, Y. H.; Lee, S.-H.; Lim, S.; Noh, S.-K.; Kim, Y.-H.; Kahng, S.-J. Visualizing Tilted Binding and Precession of Diatomic NO Adsorbed to Co-Porphyrin on Au (111) Using Scanning Tunneling Microscopy. *Chem. Sci.* **2014**, *5*, 2224–2229.
20. Zhang, J. L.; Wang, Z.; Zhong, J. Q.; Yuan, K. D.; Shen, Q.; Xu, L. L.; Niu, T. C.; Gu, C. D.; Wright, C. A.; Tadich, A.; et al. Single-Molecule Imaging of Activated Nitrogen Adsorption on Individual Manganese Phthalocyanine. *Nano Lett.* **2015**, *15*, 3181–3188.
21. Stipe, B.; Rezaei, M.; Ho, W.; Gao, S.; Persson, M.; Lundqvist, B. Single-Molecule Dissociation by Tunneling Electrons. *Phys. Rev. Lett.* **1997**, *78*, 4410.
22. Foley, E.; Kam, A.; Lyding, J.; Avouris, P. Cryogenic UHV-STM Study of Hydrogen and Deuterium Desorption from Si(100). *Phys. Rev. Lett.* **1998**, *80*, 1336.
23. Stokbro, K.; Thirstrup, C.; Sakurai, M.; Quaade, U.; Hu, B. Y.-K.; Perez-Murano, F.; Grey, F. STM-Induced Hydrogen Desorption *via* a Hole Resonance. *Phys. Rev. Lett.* **1998**, *80*, 2618.
24. Sloan, P.; Hedouin, M.; Palmer, R.; Persson, M. Mechanisms of Molecular Manipulation with the Scanning Tunneling Microscope at Room Temperature: Chlorobenzene/S I (111)-(7× 7). *Phys. Rev. Lett.* **2003**, *91*, 118301.
25. Sloan, P. A.; Palmer, R. Two-Electron Dissociation of Single Molecules by Atomic Manipulation at Room Temperature. *Nature* **2005**, *434*, 367–371.
26. Martel, R.; Avouris, P.; Lyo, I.-W. Molecularly Adsorbed Oxygen Species on Si (111)-(7× 7): STM-Induced Dissociative Attachment Studies. *Science* **1996**, *272*, 385–388.
27. Shen, T.-C.; Wang, C.; Abeln, G.; Tucker, J.; Lyding, J.; Avouris, P.; Walkup, R. Atomic-Scale Desorption through Electronic and Vibrational Excitation Mechanisms. *Science* **1995**, *268*, 1590–1592.
28. Shin, H.-J.; Jung, J.; Motobayashi, K.; Yanagisawa, S.; Morikawa, Y.; Kim, Y.; Kawai, M. State-Selective Dissociation of a Single Water Molecule on an Ultrathin MgO Film. *Nat. Mater.* **2010**, *9*, 442–447.
29. Yoder, N.; Guisinger, N.; Hersam, M.; Jorn, R.; Kaun, C.-C.; Seideman, T. Quantifying Desorption of Saturated Hydrocarbons from Silicon with Quantum Calculations and Scanning Tunneling Microscopy. *Phys. Rev. Lett.* **2006**, *97*, 187601.
30. Kresse, G.; Furthmüller, J. Efficiency of Ab-Initio Total Energy Calculations for Metals and Semiconductors Using a Plane-Wave Basis Set. *Comput. Mater. Sci.* **1996**, *6*, 15–50.
31. Woo, S.-J.; Lee, E.-S.; Yoon, M.; Kim, Y.-H. Finite-Temperature Hydrogen Adsorption and Desorption Thermodynamics Driven by Soft Vibration Modes. *Phys. Rev. Lett.* **2013**, *111*, 066102.
32. Blöchl, P. E. Projector Augmented-Wave Method. *Phys. Rev. B: Condens. Matter Mater. Phys.* **1994**, *50*, 17953–17979.
33. Perdew, J. P.; Burke, K.; Ernzerhof, M. Generalized Gradient Approximation Made Simple. *Phys. Rev. Lett.* **1996**, *77*, 3865–3868.
34. Grimme, S. Semiempirical GGA-Type Density Functional Constructed with a Long-Range Dispersion Correction. *J. Comput. Chem.* **2006**, *27*, 1787–1799.
35. Chase, M.; Davies, C.; Downey, J.; Frurip, D. JANAF Thermochemical Tables Third Edition. *J. Phys. Chem. Ref. Data* **1985**, *14*, 1735–1740.
36. Reuter, K.; Scheffler, M. Composition, Structure, and Stability of RuO_2 (110) as a Function of Oxygen Pressure. *Phys. Rev. B: Condens. Matter Mater. Phys.* **2001**, *65*, 035406.
37. Kim, Y.-H.; Heben, M. J.; Zhang, S. B. Nanotube Wires on Commensurate Inas Surfaces: Binding Energies, Band Alignments, and Bipolar Doping by the Surfaces. *Phys. Rev. Lett.* **2004**, *92*, 176102.